

ATOMIC MECHANISM OF THE INFLUENCE OF ELASTIC DEFORMATIONS IN EPITAXIAL Ge LAYERS ON THE SURFACE Si(111) ON THE DIFFUSION OF Ge ADATOMS

© 2024 R. A. Zhachuk*

*Rzhanov Institute of Semiconductor Physics, Siberian Branch of the Russian Academy of Sciences
630090, Novosibirsk, Russia
e-mail: zhachuk@gmail.com

Received February 13, 2024

Revised April 01, 2024

Accepted April 02, 2024

Abstract. Using density functional theory calculations, the atomic mechanism of the influence of compressive strains formed on the Ge(111) – 7×7 surface of epitaxial layers, grown on Si(111) substrate, on the diffusion of Ge adatoms was investigated. It was found that the energy barrier limiting the migration of Ge adatoms over long distances is located near corner vacancies of the 7×7 structure and is caused by the formation of a covalent bond between the Ge adatom and a dimer atom within the 7×7 structure. It is shown that the barrier increase on the elastically compressed surface occurs due to strengthening of the dimer bond during surface compression, which leads to weakening of the bond between the Ge adatom and the dimer atom.

DOI: 10.31857/S004445102408e08X

1. INTRODUCTION

The diffusion of adatoms on crystal surfaces has a direct impact on the growth of thin films, their morphology, and the formation of nanostructures, and is therefore an important research topic. One of the factors that can influence adatom diffusion is elastic deformation of the surface lattice.

It has been previously demonstrated experimentally that the activation energy for adatom diffusion on metal surfaces decreases with lateral compression of the surface lattice, and the mechanism of this phenomenon has been theoretically studied [1, 2]. It was found that when metal surfaces are compressed, adatoms are positioned farther from the surface and therefore have a less corrugated potential.

However, the dependence of diffusion activation energy on the sign of lattice deformation on the surfaces of covalent crystals, such as Si or Ge, may have a more complex nature due to directional and localized bonds between adatoms and surface atoms. One of the most studied elastically strained systems is Ge on the Si surface. This is due to the fact that nanostructures formed on the basis of Ge/Si are promising for application in optoelectronic devices [3]. The lattice constant of Ge is approximately 4%

larger than Si, and therefore Ge layers grown on the Si surface are laterally compressed.

Previously, Cherepanov and Voigtlander experimentally showed that the activation energies for diffusion of Ge adatoms on the surface of layers Ge(111) – 7×7 , grown on Si(111), increase under lattice compression [4, 5]. However, no explanation for this phenomenon was given. The aim of this work was to determine the atomic mechanism of increasing the activation energy of surface self-diffusion Ge(111) – 7×7 under compression.

2. CALCULATION DETAILS

To study the dynamics of Ge adatom on the surface Ge(111), the potential energy surface for this atom was calculated based on density functional theory. The calculation used a commonly accepted model of the structure 7×7 , consisting of dimers, adatoms, and stacking faults (dimers – adatoms – stacking faults, DAS) [6].

It is known that this structure is stable on the surface Ge(111) within a certain range of compression deformations [7, 8]. The calculations were performed using the SIESTA software package, which uses atomic orbitals as basis functions [9]. An

exchange-correlation functional in the generalized gradient approximation (GGA) was used [10]. To describe the valence electrons of Ge atoms, two sets of s - and p -orbitals and one set of d -orbitals were used (13 functions per atom). Other calculation details are similar to those we previously used to study Sr atom diffusion on the surface Si(111) – 7×7 [11].

To calculate the dependence of the potential energy of a Ge adatom on its position in the cell 7×7 of the surface, this atom was placed at a height of approximately 3\AA above the surface Ge(111). The z atom coordinate (in the direction perpendicular to the surface) could freely change, while the coordinates in the xy plane were fixed. The system relaxed until the forces acting on the atoms became less than 0.01 eV/\AA . As a result, a potential energy surface was obtained for the adsorbed atom $E(x, y)$.

The distance between the nodes of the hexagonal surface lattice, at which the potential energy values were calculated, was approximately 0.6 \AA . The exact values of local minima energies $E(x, y)$ were calculated using a freely moving Ge adatom placed near the local minimum of the potential energy surface. The calculation error of energy barriers, caused by the finite distance between the hexagonal lattice nodes, did not exceed 0.1 eV .

3. RESULTS

Figs. 1a, b show the calculated potential energy surfaces $E(x, y)$ for a Ge adatom on unstrained and elastically compressed by 4% surfaces Ge(111) – 7×7 . Light (dark) areas correspond to low (high) system energy respectively. The relative energies of adatom local minima (numbered from 1 to 6) on these surfaces, located in the unfaulted u and faulted f halves of the cell 7×7 , are shown in the table. It can be seen that the local energy minima of the surface are located near adatoms and rest-atoms of the structure 7×7 , where the adsorbed atom can saturate several dangling bonds at once surface. Visual inspection of the relaxed crystal lattice showed that the energy minima on the undeformed surface (1–4 in Fig. 1a) are associated with the formation of ad-dimers in positions T_4 . These ad-dimers consist of an adatom in the 7×7 structure and an additional adsorbed (diffusing) Ge atom. Such arrangement of stable adsorption sites corresponds to that previously found in a system with similar properties Si/Si(111) – 7×7 [12]. When the surface is compressed, some of these minima disappear, but new ones appear instead (5 and 6 in Fig. 1b).

Table. Relative energies (eV) of Ge adatom local minima on the surface Ge(111) – 7×7 . N – minimum number according to Fig. 1a, b indices u and f refer to *unfaulted* and *faulted* halves of the cells 7×7 . For each surface (unstrained and elastically compressed by 4%) the energy scale starts from the energy of the deepest minimum

N	Unstrained		Elastically compressed	
	u	f	u	f
1	0.22	0.11	–	0.26
2	0.07	0.00	0.21	
3	0.15	0.12	–	–
4	0.09	0.11	–	–
5	–	–		0.15
6	–	–	0.15	0.0

The calculation showed that the energy barriers between individual potential energy minima in the cell 7×7 are low ($0.2\text{--}0.3 \text{ eV}$). This is due to the high concentration of dangling bonds on the surface in this area, located on adatoms and rest atoms. Therefore, during adatom migration, the formation of new bonds and breaking of old ones occur simultaneously, leading to low energy barriers. However, to overcome cell boundaries 7×7 for long-distance adatom diffusion, it needs to pass a rather high barrier located above the dimer rows along the cell perimeter 7×7 . The formation of a high energy barrier in this area is caused by the fact that all bonds in the dimers of structure 7×7 are saturated, and therefore the adatom needs to significantly weaken its bond with the surface. The transition frequency of the adatom (ν) through the energy barrier (E_b), according to the Arrhenius equation, exp exponentially depends on the magnitude of this barrier $\nu = \nu_0 \exp(-E_b/k_B T)$, where T is temperature, k_B is Boltzmann constant, and the pre-exponential factor ν_0 describes the frequency of jump attempts over the energy barrier and depends on local crystal lattice vibrations. Thus, according to the potential energy surface reliefs shown in Fig. 1a, b, the adatom will move relatively quickly within the cell 7×7 , jumping between different local energy minima, while jumps to adjacent superstructure cells 7×7 will occur much less frequently. This phenomenon was previously observed for other systems [13–20].

In Fig. 1a, one can see that the lowest energy barriers between cell halves 7×7 are observed above dimer atoms, with the barrier above the dimer atom located near the corner vacancy of structure 7×7 being the lowest.

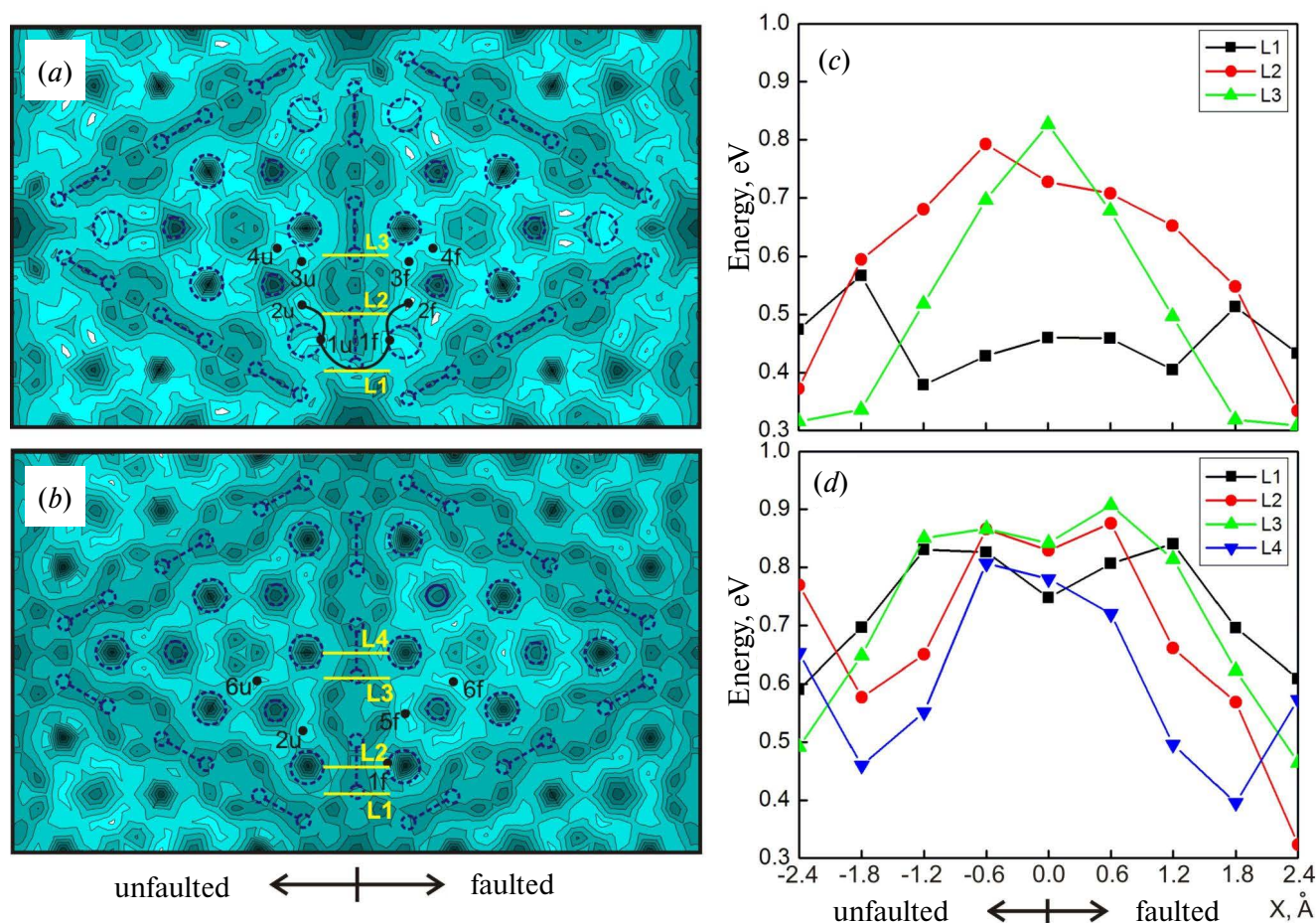


Fig. 1. *a, b* – Potential energy surface relief $E(x, y)$ for Ge atom on the surface $\text{Ge}(111) - 7 \times 7$. Contour lines are placed with 0.2 eV energy step. Light (dark) areas correspond to low (high) energy. Structure elements 7×7 are highlighted with dashed lines: large circles – adatoms, medium – rest atoms, dumbbells – dimers. Numbered points (*u* or *f*) indicate locations of local minima in the unfaulted and faulted halves of the cell 7×7 . Light lines (L1-L4) indicate the positions of calculated adatom migration paths between cell halves 7×7 . The solid dark line between minima 2*u* and 2*f* in Fig. *a* – minimum energy path (MEP) for long-distance adatom migration. *a* – Undeformed surface. *b* – Elastically compressed 4% surface. *c, d* – Potential energy surface profiles along L1-L4 lines on undeformed (*c*) and elastically compressed (*d*) $\text{Ge}(111) - 7 \times 7$ surfaces. For each surface, the energy scale starts from the deepest minimum (2*f* for undeformed and 6*f* for elastically compressed surfaces)

It was found that this is caused by the formation of weak covalent bonds between the adatom and dimer atoms. Interestingly, bond formation occurs despite the fact that formally all bonds in the dimers of structure 7×7 are closed. Indeed, in Fig. 2*a*, one can see that when a Ge adatom is adsorbed above a dimer atom, there is electron density between them indicating the formation of a covalent bond. Fig. 1*c* shows the calculated potential energy surface profiles along lines L1-L3 in Fig. 1*a* above dimer atoms. It can be seen that the profile along line L1 has a barrier height of 0.4–0.5 eV, while for lines L2 and L3 the barrier height is 0.7–0.8 eV. Thus, the minimum energy path (MEP) for Ge adatom diffusion over long distances runs along the dark curve connecting minima 2*u* and 2*f*. The saddle point of this path

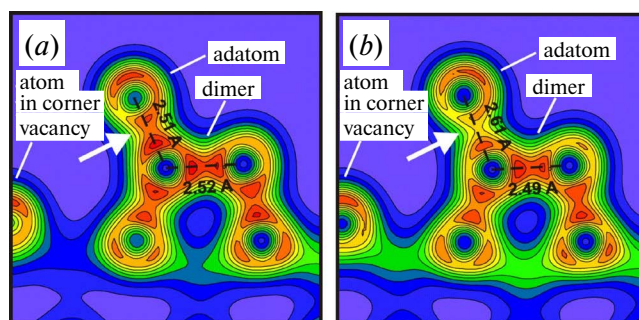


Fig. 2. Vertical cross-section of valence electron density for a Ge adatom adsorbed in the center of line L1 in Fig. 1*a, b* (cross-section along the dimer row of structure 7×7). *a* – Undeformed surface. *b* – Elastically compressed by 4% surface. The arrow shows the covalent bond forming between the Ge adatom and the dimer atom. Bond lengths are indicated in angstroms

is located above the dimer atom near the corner vacancy, and the barrier height determines the activation energy of diffusion.

A question may arise why the barriers along lines L2 and L3 in Fig. 1*a, b* are higher than along L1, although all lines pass over dimer atoms. It is known that bonds in dimers of structure 7×7 on the undeformed surface Ge(111) are stretched relative to bonds in the crystal bulk [21]. Thus, bonds in dimers located near corner vacancies of structure 7×7 are longer than bonds in the crystal bulk by approximately 4%, while bonds in dimers located midway between vacancies are less stretched (about 3%). Additionally, for the dimer atom near the corner vacancy, the largest deviation of bond angles from the value 109.5° , characteristic of diamond-type lattice, is observed. Thus, sp^3 -hybridization of electronic shells of the dimer atom nearest to the corner vacancy is most strongly distorted, and this likely promotes the formation of a weak covalent bond with the Ge adatom.

When the surface is compressed by 4% in the lateral direction, the MEP path along line L1 becomes significantly blocked (Fig. 1*b*). Indeed, the energy barrier along L1 on the potential energy surface profile in Fig. 1*d* is comparable to the barrier height along lines L2 – L4 and it is approximately 0.8 eV.

The energy barrier is the energy difference between the saddle point and the global minimum of the potential energy surface. Thus, the increase in the energy barrier along the L1 line on the surface Ge(111) during its compression can be caused by both the formation of stronger bonds in the global minimum 6*f* in the cell 7×7 (table), and the weakening of the adatom's bond with the surface at the saddle point during adsorption on the dimer atom (or both factors together). However, there is a difficulty here related to the fact that the energies of the Ge adatom on undeformed and elastically compressed surfaces Ge(111) – 7×7 cannot be compared directly. To solve this problem, we referenced the calculated energies to the common vacuum level. Thus, the adsorption energies of the Ge adatom were calculated at the global energy minima in the cell 7×7 and saddle points along the L1 lines. It was found that the adsorption energy at global energy minima is approximately the same for undeformed and elastically compressed surfaces. In contrast, the adsorption energy at the L1 saddle point for the elastically compressed surface Ge(111) is lower than for the undeformed one by approximately 0.28 eV. Consequently, the increase in the energy barrier along L1 during surface compression is caused by the

weakening of the Ge adatom's bond with the surface at the saddle point (above the dimer atom).

Fig. 2*b* illustrates the atomic mechanism of this phenomenon. Surface compression Ge(111) leads to a reduction in the length of the initially stretched bond between dimer atoms. Thus, the length of this bond becomes closer to the equilibrium length for bulk Ge. This is accompanied by an increase in the bond length between the Ge adatom and the dimer atom. Shortening/lengthening of the bond means strengthening/weakening of the corresponding atomic bonds. In Fig. 2*b* one can see that this process is accompanied by redistribution of electron density from the weakening σ -bond between atoms to the one that becomes stronger.

From general considerations, it is clear that the picture of monomer diffusion considered in this work will be valid at low concentrations of adsorbed Ge adatoms, when each diffusing atom can be considered independently. Studying the diffusion of adatom clusters on the surface using density functional theory calculations currently presents a very complex task requiring enormous computational time. Previously, several experimental works discussed the contribution of "magic" Si clusters formed on the surface Si(111) – 7×7 to self-diffusion and homoepitaxial growth [22–24]. However, in the work of Cherepanov and Voigtländer [4], it was shown that the contribution of "magic" Ge clusters to diffusion and formation of two-dimensional islands on the surface Ge(111) in the temperature range 400–700 K is absent. This conclusion is based on the fact that the density of "magic" clusters on the surface Ge(111) with structure 7×7 is much higher than on the same surface with structure 5×5 , however, the concentration of two-dimensional islands formed during Ge growth does not depend on the surface structure.

According to the above-described mechanism of energy barrier formation at the boundary of structure cells 7×7 , a barrier of similar magnitude should be observed at the boundary of cells 5×5 . This occurs due to the local nature of adatom-surface interaction on one hand, and identical local atomic structure in reconstructions 5×5 and 7×7 on the other. Thus, the theoretical data presented above agree both with the absence of dependence of germanium diffusion rate on surface structure Ge(111), and with the increase in energy barrier during surface compression, obtained from experiment [4]. These facts, as well as conclusions about the absence of contribution from "magic" Ge clusters to diffusion and formation of two-dimensional islands on the Ge(111) surface, made in the work of Cherepanov and Voigtländer

[4], indicate that Ge monomer diffusion takes place on the surface Ge(111) – 7×7 .

4. CONCLUSIONS

The influence of elastic deformations of the surface Ge(111) – 7×7 , occurring during Ge growth on the substrate Si(111) on the diffusion of Ge atoms has been investigated. It has been shown that the diffusion rate of a Ge adatom on an undeformed surface Ge(111) – 7×7 is determined by the energy barrier located at the cell boundary 7×7 above the dimer atoms near the corner vacancies of the structure 7×7 . It has been established that surface compression strengthens the bonds between the dimer atoms of the structure 7×7 . This leads to the weakening of the bond between the dimer and the adatom due to the redistribution of electron density from this bond to the bond between dimer atoms. The weakening of the Ge adatom bond with the surface results in an increase in the diffusion activation energy. The results of this work can find application in optimizing the growth processes of thin films and Ge nanostructures on the Si surface.

ACKNOWLEDGMENTS

The author expresses gratitude to the NSU Computing Center for providing access to the cluster computing resources.

FUNDING

This work was supported by the Russian Science Foundation (project No. 19-72-30023).

REFERENCES

1. H. Brune, K. Bromann, H. Röder, K. Kern, J. Jacobsen, P. Stoltze, K. Jacobsen, and J. Nørskov, *Phys. Rev. B* **52**, R14380(R) (1995).
2. C. Ratsch, A. P. Seitsonen, and M. Scheffler, *Phys. Rev. B* **55**, 6750 (1997).
3. O.P. Pchelyakov, A.V. Dvurechensky, A.V. Latyshev, and A.L. Aseev, *Semicond. Sci. Technol.* **26**, 014027 (2010).
4. V. Cherepanov and B. Voigtländer, *Phys. Rev. B* **69**, 125331 (2004).
5. V. Cherepanov and B. Voigtländer, *Appl. Phys. Lett.* **81**, 4745 (2002).
6. K. Takayanagi, Y. Tanishiro, S. Takahashi, and M. Takahashi, *Surf. Sci.* **164**, 367 (1985).
7. H.J. Gossmann, J.C. Bean, L.C. Feldman, E.G. McRae, and I.K. Robinson, *Phys. Rev. Lett.* **55**, 1106 (1985).
8. R. Zhachuk, S. Teys, and J. Coutinho, *J. Chem. Phys.* **138**, 224702 (2013).
9. J.M. Soler, E. Artacho, J.D. Gale, A. García, J. Junquera, P. Ordejón, and D. Sanchez-Portal, *J. Phys. Condens. Matter* **14**, 2745 (2002).
10. J.P. Perdew, K. Burke, and M. Ernzerhof, *Phys. Rev. Lett.* **77**, 3865 (1996).
11. R.A. Zhachuk, S.A. Teys, B.Z. Olshanetsky, *JETP* **140**, 1113 (2011).
12. C.M. Chang and C.M. Wei, *Phys. Rev. B* **67**, 033309 (2003).
13. R. Zhachuk, S. Teys, B. Olshanetsky, and S. Pereira, *Appl. Phys. Lett.* **95**, 061901 (2009).
14. T. Sato, S.I. Kitamura, and M. Iwatsuki, *Surf. Sci.* **445**, 130 (2000).
15. H. Uchida, T. Kuroda, F.B. Mohamad, J. Kim, K. Kashiwagi, K. Nishimura, and M. Inoue, *Phys. Stat. Sol.* **241**, 1665 (2004).
16. L. Vitali, M.G. Ramsey, and F.P. Netzer, *Phys. Rev. Lett.* **83**, 316 (1999).
17. O. Custance, I. Brihuega, J.M. Gómez-Rodríguez, and A.M. Baró, *Surf. Sci.* **482–485**, 1406 (2001).
18. O. Custance, S. Brochard, I. Brihuega, E. Artacho, J.M. Soler, A.M. Baró, and J.M. Gómez-Rodríguez, *Phys. Rev. B* **67**, 235410 (2003).
19. J. Mysliveček, P. Sobotík, I. Ošťádal, T. Jarolímek, and P. Šmilauer, *Phys. Rev. B* **63**, 045403 (2001).
20. C. Polop, E. Vasco, J.A. Martín-Gago, and J.L. Sacedón, *Phys. Rev. B* **66**, 085324 (2002).
21. A.E. Dolbak, R.A. Zhachuk, *JETP* **160**, 55 (2021).
22. I.S. Hwang, M.S. Ho, and T.T. Tsong, *Phys. Rev. Lett.* **83**, 120 (1999).
23. I.S. Hwang, M.S. Ho, and T.T. Tsong, *Surf. Sci.* **514**, 309 (2002).
24. M.S. Ho, I.S. Hwang, and T.T. Tsong, *Surf. Sci.* **564**, 93 (2004).